

A MINIATURIZED DIELECTRIC RESONATOR ANTENNA USING METASURFACE WITH MICROSTRIP FEEDING

Kaviya.S,Nishana.S,Pandeeswari.P (Student Members),

Electronics and Communication of K.L.N College of Engineering (Autonomous affiliated to Anna university),Madurai,
India kavivashankar0212@gmail.com , nishaselva0506@gmail.com , angalaeswaripandiarajan@gmail.com

Abstract — A miniaturized Rectangular Dielectric Resonator Antenna loaded with metasurface is proposed here. The metasurface is stacked with unit cells in 4x4 structure. The DRA is placed over the PEC (emits Transverse electrical waves) where as the Port 1 and Port 2 is etched at the sides of the DRA adjacent to the two PMC (emits transverse mechanical waves) boards along the DRA. The substrate is sandwiched between copper patch and the ground plane to provide insulation, reducing its interference and ensuring signal integrity. The microstrip feeding is fed over the substrate with the radiation bandwidth 2-5%. Finally, the proposed structure is fabricated and tested. The DRA is resonated at a bandwidth of 3.5 GHz with S11 feature below -13.78 dB and is characterized by low cross-polarization. The simulation of the proposed antenna is done using High Frequency Structure Simulator (HFSS) software.

Keywords—Dielectric resonator antenna (DRA), minimized size, wide-bandwidth, low-profile, metasurface.

1. INTRODUCTION

Since it was first advanced in the mid 1980s [1], the dielectric resonator antenna (DRAs) have drawn consideration because of its few appealing highlights, i.e., high radiation-proficiency, little size, and high plan opportunity [2]-[5]. Tragically, the conventional DRA has a significant disadvantage of restricted data transmission as well as the microstrip antenna, particularly in a position of safety condition. In that capacity, the position of safety DRA isn't appropriate for some wide-band applications [6]. The DRA is well ahead of the MPA in terms of wider bandwidth and higher efficiency but at the cost of compromising with the gain value by approximately 1dB. It would be relevant to note that the characteristics of both types of antennas are dependent on their respective dielectric properties. During the past twenty years, a few endeavors have been made to examine and address the disadvantage of the narrow bandwidth. Firstly, an assortment of DRAs with exceptional shapes were proposed to bring down the Q-factor and thus increment their impedance data transmissions. In [7] and [8], both antenna types are very close in some aspects as they both have similar feed mechanisms and radiation patterns. Although they have their individual merit and potential, very few works so far have addressed comparative study between the DRA and the microstrip patch antenna altered ventured pyramidal shape and T-shape were acquainted with accomplishing a wideband property of over 60%. This approach expanded the plan intricacy or profile of the DRAs. Likewise, the

exceptional shapes additionally prompted the high cross-polarization. Besides, the DRAs with high viewpoint proportion utilizing different excitation strategies were applied to combine the prevailing mode with higher request modes. In [11], a couple of vertical microstrip lines was utilized in a perpendicular plan to energize the barrel shaped dielectric resonator receiving wire for circularly captivated execution. Unique resonators could be joined with DRAs to frame multi-full crossover receiving antenna. Sadly, these DRAs additionally experienced several basic issues, for example, prominent, huge cross over aspects or low increase. Fourthly, the DRAs with various permittivities could be upward stacked with one another to give excellent broadband execution. In any case, these stacked DRAs had prominent, high cross-polarization or asymmetrical radiation design. According to these past strategies for acknowledging broadband DRA, little consideration was all the while paid to the size-decrease of the three dimensional receiving antenna geometry and stable broad side radiation, subsequently accomplishing wanted reduced size and wide-data transmission. Lately, the metasurface (MS) has been utilized to configuration new kinds of antenna with further developed execution, like broadband and minimal size. In [16], a rectangular, semiconductor patch isolated by a hole was planned to stimulate zeroth-request resonance mode. The MS was stacked on a metasurface antenna to produce extra resonances. In this paper, a dielectric antenna with minimized geometry and upgraded bandwidth capacity is proposed. The MS structure is known with diminish the profile of the antenna and create an additional resonance of the TM surface wave mode. Moreover, a couple of Shorting walls are used to reduce the resonance frequency of the MS intending to understand the wide-transmission capacity characteristics. The proposed antenna is mathematically examined and related estimations are completed to confirm working standards and simulated results.

GEOMETRY AND WORKING PRINCIPLE

A. DRA CONFIGURATION

The configuration and parameters of the proposed DRA are portrayed in Fig. 1. It comprises of the MS (to layer), the DR (center layer), the opening coupled ground plane, and the microstrip taking care of line (base layer). For the MS, it is scratch on the top side of FR4 epoxy substrate ($\epsilon_r = 4.4$ and $\tan \delta = 0.02$). For the rectangular DR of Graphite ($\epsilon_r = 15$ and $\tan \delta = 0.0015$), it is stacked under the MS in Fig. 1(b). For the 25 microstrip taking care of line, it is put at the bottom surface of the Duroid substrate ($\epsilon_r = 2.2$ and $\tan \delta = 0.0009$).

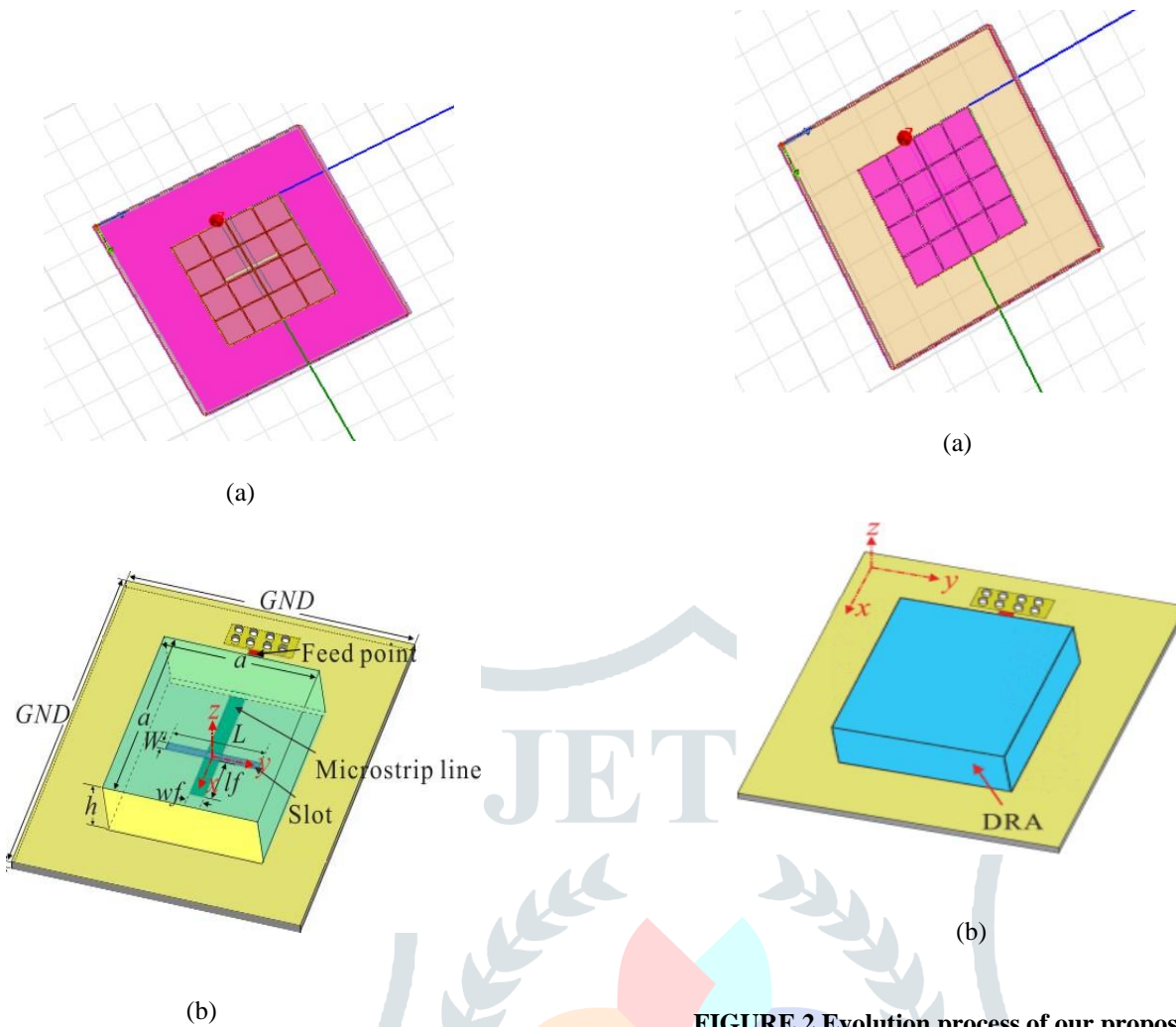


FIGURE 1. Configuration of the proposed DRA. (a). 3-D view. (b) Feeding structure and DR

FIGURE 2 Evolution process of our proposed DRA with bandwidth enhancement and miniaturization. (a). Reference antenna 2 with the MS, (b). Reference antenna 1.

B . IMPEDANCE BANDWIDTH ENHANCEMENT OF THE ANTENNA

The TE methods of the dielectric resonating receiving antenna (RDRA) under aperture coupling are profoundly examined in [19]

The particular mode can be addressed by TE_{mnp_y} , where the superscript y addresses that the part of E-field in the y-bearing is 0. In the interim, the value of m, n, and p individually address the field variety along x-, y-and z-axis. To explain the functioning standard of our proposed antenna , two reference antenna are compared about. Firstly, choosing a rectangular DR with a similar size as the reference antenna 1 is displayed in Fig. 2(b). Also, stacking the MS on the DR to decrease profile as reference rantina 2 is portrayed in Fig. 2(a). At last, the proposed DRA is developed.

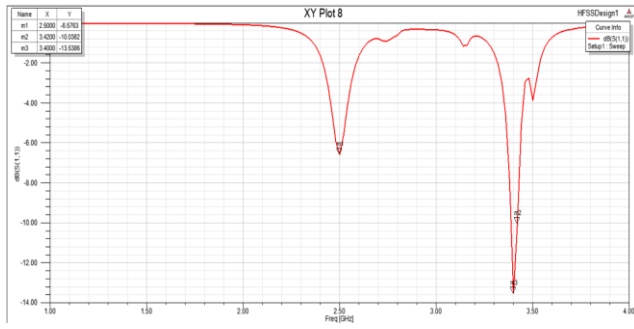


FIGURE 3. Simulated |S11| of the reference DRAs and our proposed DRA.

Design parameter	<i>h</i>	<i>h1</i>	<i>h2</i>	<i>a</i>	<i>W</i>	<i>L</i>
Value (mm)	4.66	0.67	0.17	33.3	1	18
Design parameter	<i>wf</i>	<i>lf</i>	<i>p</i>	<i>d</i>	<i>g</i>	<i>GND</i>
Value (mm)	3	21.89	8.34	8	0.34	63.34

The reproduced |S11| of the reference antenna proposed DRA. True to form, the single-mode dielectric resonator of the reference antenna 1, particularly in the low profile condition, experiences a tight data transfer capacity (1.8%). To settle this intrinsic issue, the MS structure is utilized in the reference antenna 2. Another resonance is produced, yet all at once the broadband attributes of the receiving antenna are as yet not understood. Depending on these methodologies, the impedance transmission capacity of the planned DRA. The mechanism of this peculiarity will be discussed in the following.

C. WORKING MECHANISM OF THE ANTENNA

The redistribution of different radiative modes to improve the impedance transmission capacity is applied to our proposed receiving wire [20]. Stack of rectangular patches is loaded along the non-radiative edges of the DRA. Thus, a radiative mode at the high side of the operation band is added. The dielectric waveguide model (DWM) can be used to work out the full recurrence of the customary rectangular dielectric resonating radio wire (RDRA) [21]. The resonating recurrence of TE_{111y} mode can be communicated as:

$$f_{DR} = \frac{c}{\lambda \sqrt{\epsilon_r}} = \frac{ck_0}{2\pi \sqrt{\epsilon_r}} \tag{1}$$

$$k_0 = \sqrt{k_x^2 + k_y^2 + k_z^2}, \quad k_x = \frac{\pi}{a}, \quad k_z = \frac{2\pi}{h} \tag{2}$$

$$k_y \tan\left(\frac{ak_y}{2}\right) = \sqrt{k_x^2 + k_z^2} \tag{3}$$

where,

k_x, *k_y*, and *k_z* are the wavenumbers along the x, y, and z - directions respectively.

c is the speed of light and

k₀ is the free-space wavenumber.

The fundamental mode resonant frequencies of the DRA obtained from the DWM and full-wave simulation in various sizes, indicating the error between the theoretical calculations and the full-wave simulation results is reduced. Due to the loading of metasurface the dimensions of the dielectric resonator can't be determined.. The initial height of the DR can be temporarily determined. On this basis, the design of the MS is carried out. The reference antenna 1 with the thickness of 4.66 mm is chosen as the starting point of the design. The fundamental mode TE_{111y} of the reference antenna 1 with the feed structure is excited. In the reference antenna 2, TM surface wave is excited to provide an additional radiative mode (i.e) it provides preconditions to broaden the antenna bandwidth. It is notable that the reflection stage outlines are typically used to research the reverberation attributes of the MS. The unit cell is taken on for mathematical processing of the reflection period of the metasurface. In view of the proposed aspects, the zero degree reflection stage happens at 3.43 GHz. Further, the investigation technique for surface wave resonances in [17] is presented. The resonances of the surface modes can be qualitatively determined by the following equations:

$$\beta_{sw} = \pi / L_{ms} = \pi / N \times p = \pi / N \times (d + g) \tag{4}$$

$$360^\circ / \pi \cdot \beta_{sw} p = 360^\circ / N \tag{5}$$

where,

β_{sw} is the propagation constant of the surface waves

L_{ms} is the total length of the MS.

The number of patch cells and the periodicity of the MS are *N* and *p*, respectively.

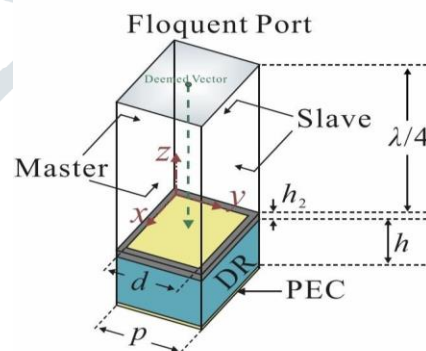


FIGURE 4 : Simulated model of the MS unit cell.

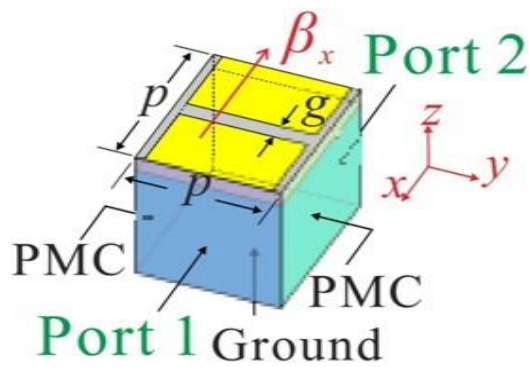


FIGURE 5. Simulation model of the MS unit cell.

As per the recreated results from (4) upon the limit condition, the scattering chart of the MS is plotted. The resonant frequencies of surface wave modes can be exactly shown by the convergences as far as the scattering bends and vertical lines addressing the worth on the right half of (5). Table 3 sums up the resonances of the TM surface wave mode acquired by the full-wave approach for the MS with various cell numbers. The outcomes portray that the quantity of MS units makes huge impacts on a superficial level wave resonances. Consequently, the suitable number of cells ought to be chosen intentionally to improve the performance of the antenna. For $N = 4$, the resonant frequency for the TM surface wave is 3.55GHz. The obtained frequency is close to the thunderous resonant frequency of the DRA mode as referenced previously, so the MS structure of 4×4 is applied to obtain wide bandwidth. The resonant frequency of the added TM surface wave is 3.50 GHz.

Benefit from the scaled down effect of the MS, the resonant frequency of the fundamental mode (TE_{y111} mode) of the DRA is diminished from 3.51 GHz to 3.42 GHz, as analyzed with the reference receiving antenna 1.

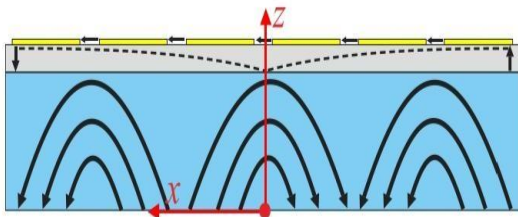


FIGURE 6. Sketch of the E-field distribution of reference antenna 2 with MS over xoz -plane at 3.75GHz.

The traditional DRA can be simplified to a RLC parallel circuit, and the resonant frequency of the DRA is determined by:

$$f_1 = 1 / 2\pi \sqrt{L_1 C_1} \quad (6)$$

Then, a new equivalent RLC circuit is added by the MS to generate a new resonance. At the same instance, the MS provides an additional load for low frequency resonance. The resonant frequency of the fundamental mode of the DRA can be further expressed by:

$$f_2 = 1 / 2\pi \sqrt{L_1 (C_1 + C_s)} \quad (7)$$

The larger capacitance implies the lower resonant frequency of the DR. Obviously, the loading of the MS excites a new resonance and reallocate the fundamental mode of the DRA. Unfortunately, the distance between the two radiative modes is still too far to realize a broad impedance bandwidth.

Our principle target is to additionally blend these two modes, intending to develop a minimized wideband DRA under dual resonance. To explain the functioning system more exhaustively, the sketch of the E-field of the reference receiving wire 2 with the MS stacked is outlined in Fig.5. The TE_{311y} mode is energized in the DRA at 3.75 GHz. Because of the use of the dielectric resonator with high dielectric constant, the interfacial surface between the dielectric and air is viewed as a magnetic plane, and the ordinary part of the electric field on its surface is zero. The resonant frequency of TM surface wave resonance is diminished from 2.42 GHz to 2.21 GHz, (i.e) the electrical size of the MS diminishes, while that of TE_{111y} mode is fundamentally unaltered.

The horizontal current is created by the MS, showing the high frequency resonance of the antenna is sensitive about the quantity of unit cells. The vertical current is induced by the E-field delivered by the horizontal current on the MS. The expansion of the ongoing way causes the transfer speed of the MS to move to bring down frequencies. At last, the redistribution of these double modes prompts the ideal broadband execution.

D. MODES AND CIRCUIT ANALYSIS OF THE ANTENNA

The simulated E-field distributions of the antenna are introduced to check the working of antenna. Fig. 6 exhibits the E-field distributions in xy -plane at the f_0 of 3.55GHz. The edge slots of the metasurface along x -axis (E-plane) produce the electromagnetic (EM) waves, showing the resonance works at a TM surface wave mode as in [22]. The metasurface antenna is introduced by well exciting both transverse magnetic (TM) wave and transverse electric (TE) wave resonances. For broadband operation the finite metasurface is utilized to excite a TM wave resonance and a TE wave resonance simultaneously for broadband operation. The obtained results of the E-field distributions of proposed DRA at xy -plane are plotted in Fig.6 that explains the low resonance is TE_{111y} mode of DR and the other is TM_{10} surface wave mode of Metasurface. The in-phase radiated field distribution are energized in two resonances. A stable radiation design with identical polarization can be kept up over the whole working bandwidth.

To confirm the design principles the whole equivalent circuit of the resonator antenna is to be developed. The impedance transformers with turn proportions equivalent to n_1 and n_2 are configured to depict the couplings of the opening to the microstrip line and the DRA to the opening [23]. Aperture-coupled antennas allows to minimize the dimensions of the rigid PEC carrying the electrical and feeding the resonator antenna. Since the aperture can be fabricated with excellent dimensional tolerances that do not change during use. Then, at that point,

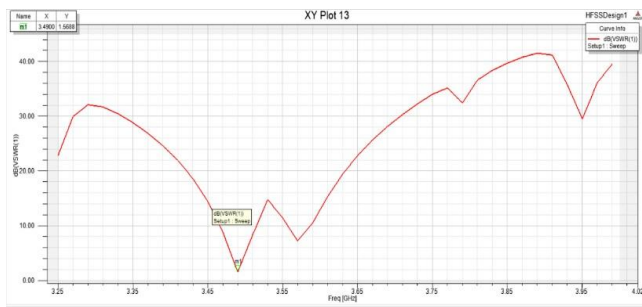


FIGURE 7: VSWR of the proposed DRA over the xoz-plane. (a). Proposed antenna of 3.45GHz to 3.55GHz.

two RLC circuits associated in series through the coupling capacitor C_o exhibit the resonances of DR and MS independently. At long last, the capacitance C_v presented by the coupling of the MS are set in with the RLC circuit of the Metasurface. The simulated $|S_{11}|$ acquired by the ADS demonstrating great concurrence with the fullwave simulation over the whole working transfer speed.

E. DESIGN GUIDELINE

Based on the above-mentioned working mechanism, a design guideline is suggested finally. It is assumed that the lower and upper frequency resonances of the antenna are f_1 and f_2 , respectively.

Step 1: Calculate the dimensions of the DR based on the DWM at f_1 .

Step 2: Set the initial height of the DR, and optimize the dimensions and the number of the MS unit cells according to the resonant frequency of the TM surface wave, i.e. f_2 .

Step 3: Set the transverse size of DR to match the size of the MS. Simulate the model to achieve the dual resonance performance of the antenna.

It should be noted that the steps 2 and 3 here in need to be debugged repeatedly to achieve optimal results.

III. EXPERIMENTAL RESULTS AND DISCUSSION S

To demonstrate the improved performance from results, a prototype of the proposed DRA with the MS loaded is fabricated and tested. The reflection coefficient ($|S_{11}|$) of the antenna is measured. The measured $|S_{11}|$ with two attenuation poles (3.43 and 3.50GHz) is consistent with the simulated one (3.44 and 3.51 GHz). As a result, the measured bandwidth of the antenna for $|S_{11}| < -10$ dB is significantly extended (3.40 – 3.45 GHz), which is wider than the traditional counterpart at the same thickness (3.4%). It is worth pointing out that the desired wide-bandwidth is acquired with a compact size.

The radiation pattern is tried by utilizing a nearfield SATIMO antenna test framework. The deliberate outcomes are in accordance with the simulation. Simultaneously, a steady typical radiation pattern with indistinguishable polarization and low cross-polarization properties is acceptably accomplished under the operation of desired double radiative resonant modes. The steady

radiation with the peak acknowledged gain of around 6.6 dBi and the radiation efficiency of around 80% is acceptably achieved in the operating bandwidth. The proposed antenna has low profile and minimized cross over aspects, while yielding a wide impedance bandwidth capacity and great radiation properties.

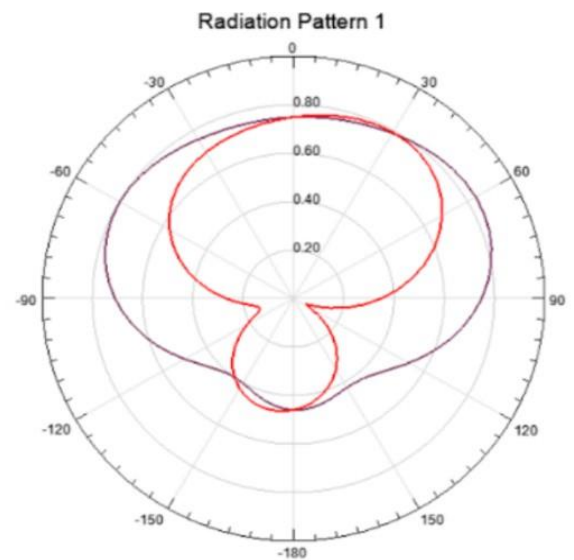


FIGURE 8: Radiation Pattern of the proposed DRA

IV. CONCLUSION

A miniaturized dielectric resonator antenna (DRA) loaded with metasurface of FR4 epoxy is proposed. The design of the 4x4 metasurface DR antenna is made and is simulated. The simulation of the proposed antenna is done by using High Frequency Structure Simulator (HFSS) Software. The proposed dielectric resonator antenna resonates at a frequency of 3.5 GHz. The proposed antenna has also achieved the s_{11} characteristics (i.e) which has to be lesser than -10 dB, where we have obtained even lesser than -13.80 dB. The applications of this antenna are Bluetooth, Long Term Evolution (LTE), World wide Interoperability for Microwave Access (WiMAX). As the frequency is increased, the size of the antenna is reduces. This can be later miniaturized if required. The Resonant frequency of the Metasurface is not achieved as expected, which is one of the wide bandwidth characteristics. This can be corrected by using a pair of shorting conducting walls on the sides of the DRA to reduce resonant frequency of the TM Surface wave mode for future applications, with these features the antenna is suitable for the wideband applications such as Satellite, Radar and Wireless communication fields.

REFERENCES

- [1] S. LONG, M. McALLISTER, AND L. SHEN, "THE RESONANT CYLINDRICAL DIELECTRIC CAVITY ANTENNA," *IEEE TRANS. ANTENNAS PROPAG.*, VOL. AP-31, NO. 3, PP. 406–412, MAY 1983.

- [2] A. A. KISHK, Y. YIN, AND A. W. GLISSON, "CONICAL DIELECTRIC RESONATOR ANTENNAS FOR WIDE-BAND APPLICATIONS," *IEEE TRANS. ANTENNAS PROPAG.*, VOL. 50, NO. 4, PP. 406–412, APR. 2002.
- [3] N. YANG AND K. W. LEUNG, "SIZE REDUCTION OF OMNIDIRECTIONAL CYLINDRICAL DIELECTRIC RESONATOR ANTENNA USING A MAGNETIC APERTURE SOURCE," *IEEE TRANS. ANTENNAS PROPAG.*, VOL. 68, NO. 4, PP. 3248–3253, APR. 2020.
- [4] N. YANG, K. W. LEUNG, AND N. WU, "PATTERN-DIVERSITY CYLINDRICAL DIELECTRIC RESONATOR ANTENNA USING FUNDAMENTAL MODES OF DIFFERENT MODE FAMILIES," *IEEE TRANS. ANTENNAS PROPAG.*, VOL. 67, NO. 11, PP. 6778–6788, NOV. 2019.
- [5] K. W. LEUNG, X. S. FANG, Y. M. PAN, E. H. LIM, K. M. LUK, AND H. P. CHAN, "DUAL-FUNCTION RADIATING GLASS FOR ANTENNAS AND LIGHT COVERS—PART II: DUAL-BAND GLASS DIELECTRIC RESONATOR ANTENNAS," *IEEE TRANS. ANTENNAS PROPAG.*, VOL. 61, NO. 2, PP. 587–597, FEB. 2013.
- [6] D. GUHA AND C. KUMAR, "MICROSTRIP PATCH VERSUS DIELECTRIC RESONATOR ANTENNA BEARING ALL COMMONLY USED FEEDS: AN EXPERIMENTAL STUDY TO CHOOSE THE RIGHT ELEMENT," *IEEE ANTENNAS PROPAG. MAG.*, VOL. 58, NO. 1, PP. 45–55, FEB. 2016.
- [7] R. CHAIR, A. A. KISHK, K. F. LEE, AND C. E. SMITH, "WIDEBAND FLIPPED STAIRED PYRAMID DIELECTRIC RESONATOR ANTENNAS," *ELECTRON. LETT.*, VOL. 40, NO. 10, PP. 581–582, MAY 2004.
- [8] Y. GAO, Z. FENG, AND L. ZHANG, "COMPACT ASYMMETRICAL T-SHAPED DIELECTRIC RESONATOR ANTENNA FOR BROADBAND APPLICATIONS," *IEEE TRANS. ANTENNAS PROPAG.*, VOL. 60, NO. 3, PP. 1611–1615, MAR. 2012.
- [9] A. RASHIDIAN, L. SHAFAI, AND D. M. KLYMYSHYN, "COMPACT WIDEBAND MULTIMODE DIELECTRIC RESONATOR ANTENNAS FED WITH PARALLEL STANDING STRIPS," *IEEE TRANS. ANTENNAS PROPAG.*, VOL. 60, NO. 11, PP. 5021–5031, NOV. 2012.
- [10] X. S. FANG, K.-P. SHI, AND Y.-X. SUN, "DESIGN OF THE SINGLE-/DUALPORT WIDEBAND DIFFERENTIAL DIELECTRIC RESONATOR ANTENNA USING HIGHER ORDER MODE," *IEEE ANTENNAS WIRELESS PROPAG. LETT.*, VOL. 19, NO. 9, PP. 1605–1609, SEP. 2020.
- [11] R. CHOWDHURY, N. MISHRA, M. M. SANI, AND R. K. CHAUDHARY, "ANALYSIS OF A WIDEBAND CIRCULARLY POLARIZED CYLINDRICAL DIELECTRIC RESONATOR ANTENNA WITH BROADSIDE RADIATION COUPLED WITH SIMPLE MICROSTRIP FEEDING," *IEEE ACCESS*, VOL. 5, PP. 19478–19485, 2017.
- [12] A. BUERKLE, K. SARABANDI, AND H. MOSALLAEI, "COMPACT SLOT AND DIELECTRIC RESONATOR ANTENNA WITH DUAL-RESONANCE, BROADBAND CHARACTERISTICS," *IEEE TRANS. ANTENNAS PROPAG.*, VOL. 53, NO. 3, PP. 1020–1027, MAR. 2005.
- [13] NASIMUDDIN AND K. P. ESSELLE, "A LOW-PROFILE COMPACT MICROWAVE ANTENNA WITH HIGH GAIN AND WIDE BANDWIDTH," *IEEE TRANS. ANTENNAS PROPAG.*, VOL. 55, NO. 6, PP. 1880–1883, JUN. 2007.
- [14] Y. GE, K. P. ESSELLE, AND T. S. BIRD, "COMPACT DIELECTRIC RESONATOR ANTENNAS WITH ULTRAWIDE 60%–110% BANDWIDTH," *IEEE TRANS. ANTENNAS PROPAG.*, VOL. 59, NO. 9, PP. 3445–3448, SEP. 2011.
- [15] Y. M. PAN AND S. Y. ZHENG, "A LOW-PROFILE STACKED DIELECTRIC RESONATOR ANTENNA WITH HIGH-GAIN AND WIDE BANDWIDTH," *IEEE ANTENNAS WIRELESS PROPAG. LETT.*, VOL. 15, PP. 68–71, 2016.
- [16] N. MISHRA AND R. K. CHAUDHARY, "A MINIATURIZED ZOR ANTENNA WITH ENHANCES BANDWIDTH FOR WiMAX APPLICATIONS," *MICROW. OPT. TECHNOL. LETTER.*, VOL. 58, NO. 1, PP. 71–75, JAN. 2016.
- [17] S. X. TA AND I. PARK, "LOW-PROFILE BROADBAND CIRCULARLY POLARIZED PATCH ANTENNA USING METASURFACE," *IEEE TRANS. ANTENNAS PROPAG.*, VOL. 63, NO. 12, PP. 5929–5934, DEC. 2015.
- [18] N.-W. LIU, L. ZHU, W.-W. CHOI, AND X. ZHANG, "A LOW-PROFILE APERTURECOUPLED MICROSTRIP ANTENNA WITH ENHANCED BANDWIDTH UNDER DUAL RESONANCE," *IEEE TRANS. ANTENNAS PROPAG.*, VOL. 65, NO. 13, PP. 1055–1061, MAR. 2017.
- [19] R. K. MONGIA, A. ITTIBIPOON, AND M. CUHACI, "LOW PROFILE DIELECTRIC RESONATOR ANTENNAS USING A VERY HIGH PERMITTIVITY MATERIAL," *ELECTRON. LETT.*, VOL. 30, NO. 17, PP. 1362–1363, AUG. 1994.
- [20] N. LIU, L. ZHU, AND W. CHOI, "A DIFFERENTIAL-FED MICROSTRIP PATCH ANTENNA WITH BANDWIDTH ENHANCEMENT UNDER OPERATION OF TM₁₀ AND TM₃₀ MODES," *IEEE TRANS. ANTENNAS PROPAG.*, VOL. 65, NO. 4, PP. 1607–1614, APR. 2017.
- [21] R. K. MONGIA AND A. ITTIBIPOON, "THEORETICAL AND EXPERIMENTAL INVESTIGATIONS ON RECTANGULAR DIELECTRIC RESONANT ANTENNAS," *IEEE TRANS. ANTENNAS PROPAG.*, VOL. 45, NO. 9, PP. 1348–1359, SEP. 1997.
- [22] W. E. I. LIU, Z. N. CHEN, AND X. QING, "BROADBAND LOW-PROFILE L-PROBE FED METASURFACE ANTENNA WITH TM LEAKY WAVE AND TE SURFACE WAVE RESONANCES," *IEEE TRANS. ANTENNAS PROPAG.*, VOL. 68, NO. 3, PP. 1348–1355, MAR. 2020.
- [23] J. ZHANG, S. YAN, AND G. A. E. VANDENBOSCH, "A MINIATURE FEEDING NETWORK FOR APERTURE-COUPLED WEARABLE ANTENNAS," *IEEE TRANS. ANTENNAS PROPAG.*, VOL. 65, NO. 5, PP. 2650–2654, MAY 2017.